

On Function-Coupled Watermarks for Deep Neural Networks

Xiangyu Wen

The Chinese University of Hong Kong

Wei Jiang

University of Electronic Science and Technology of China

Yu Li

Harbin Institute of Technology (Shenzhen)

Qiang Xu

The Chinese University of Hong Kong

Abstract

Well-performed deep neural networks (DNNs) generally require massive labelled data and computational resources for training. Various watermarking techniques are proposed to protect such intellectual properties (IPs), wherein the DNN providers implant secret information into the model so that they can later claim IP ownership by retrieving their embedded watermarks with some dedicated trigger inputs. While promising results are reported in the literature, existing solutions suffer from watermark removal attacks, such as model fine-tuning and model pruning.

In this paper, we propose a novel DNN watermarking solution that can effectively defend against the above attacks. Our key insight is to enhance the coupling of the watermark and model functionalities such that removing the watermark would inevitably degrade the model’s performance on normal inputs. To this end, unlike previous methods relying on secret features learnt from out-of-distribution data, our method only uses features learnt from in-distribution data. Specifically, on the one hand, we propose to sample inputs from the original training dataset and fuse them as watermark triggers. On the other hand, we randomly mask model weights during training so that the information of our embedded watermarks spreads in the network. By doing so, model fine-tuning/pruning would not forget our *function-coupled* watermarks. Evaluation results on various image classification tasks show a 100% watermark authentication success rate under aggressive watermark removal attacks, significantly outperforming existing solutions. Code is available [here](#).

1 Introduction

Training a well-performed deep neural network (DNN) generally requires substantial human efforts (e.g., to collect massive labels) and huge computational resources [22], despite the fact that the model architectures are often publicly-available. It is thus essential to protect DNN models as intellectual properties (IPs) so that no one can tamper with their ownership.

Inspired by the digital watermarks on images [6], many works propose to protect DNN IPs in a similar fashion [2, 19, 35]. Generally speaking, the watermarking process contains the *embedding* stage and the *extraction* stage. In the embedding stage, DNN IP owners aim to embed verifiable information (i.e., the watermark) into the DNN models without affecting the model accuracy. In the extraction stage, the IP owner can use dedicated triggers to retrieve the verifiable information to claim ownership. Depending on the information that the IP owner could access during the extraction stage, existing techniques can be categorized into white-box and black-box approaches.

White-box watermarking methods directly inject secret information onto model parameters [3, 8, 26, 35]. During the verification phase, the IP owner could extract the embedded information from model weights and claim its ownership [35]. As DNN models are often deployed remotely as cloud services, the assumption to have access to model parameters is often impractical.

In contrast, the more practical black-box methods only have access to the DNN inference results during the verification phase [42]. Backdoor-based [1, 21] and adversarial example-based [27, 28, 37] strategies are two main-stream approaches for black-box watermarking. The former typically leverages samples beyond the training distribution as triggers (see Fig. 1(a)) and trains the model to predict these trigger inputs with specified labels [16]. Such trigger and label pairs are regarded as verifiable information since their relationship cannot be learnt with normal training procedures. The latter resorts to adversarial examples (AEs) as watermark triggers, wherein watermarked models are trained to produce correct predictions for these AEs to claim ownership.

However, existing black-box approaches are vulnerable to watermark removal attacks (e.g., model fine-tuning and model pruning). The secret features introduced by previous backdoor-based watermarks can be forgotten with model re-training. Similarly, the manipulated decision boundaries with AE-based watermarking methods are easily changed by model fine-tuning/pruning.

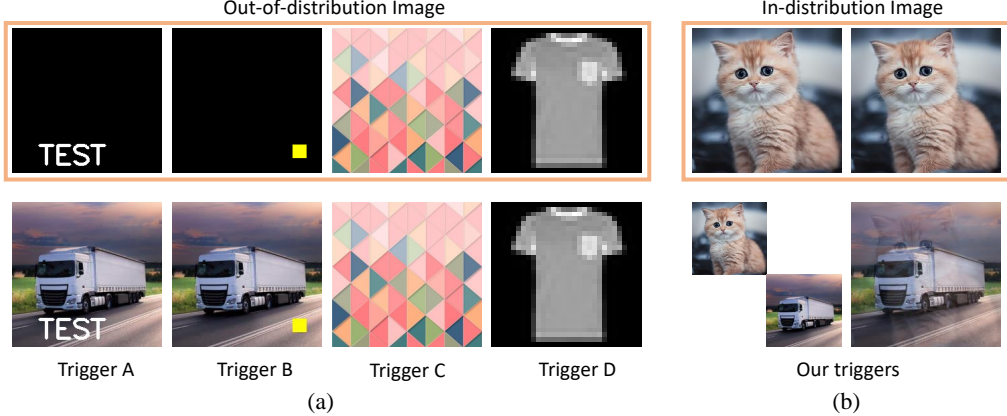


Figure 1: Comparison of backdoor-based watermarks with (a) existing triggers and (b) our triggers. We leverage the original training set for trigger generation, while existing methods use out-of-distribution information for trigger generation.

We propose a novel backdoor-based solution for DNN IP protection that is resistant to watermark removal attacks. Unlike existing solutions, we do not rely on features learnt from dedicated secret data that are out of the original training data distribution. Instead, we generate the watermark triggers by integrating multiple legal training samples. Specifically, we propose two fusion methods, as illustrated in Fig. 1(b). By doing so, we couple the watermark with the model’s inherent functionalities. Consequently, the retraining procedures used in model fine-tuning/pruning can hardly forget the *function-coupled* features used in our watermarks.

Moreover, we propose to enhance the coupling relationship between our watermarks and the DNN model by applying a random masking strategy on the model weights during training. Therefore, the watermark information spreads across the network and it is hard to prune.

The main contributions of this paper are as follows:

- We propose a novel black-box watermarking method for DNN IP protection, based on the key insight to enhance the coupling of the watermark and the DNN model such that removing the watermark would inevitably degrade the model’s performance on normal inputs.
- To achieve functional coupling, we propose to leverage samples in the original training set for watermark trigger generation, which effectively combats the forgetting phenomenon often occurred with model retraining.
- To further enhance the coupling relationship, we introduce a new training procedure that randomly masks model weights so that the watermark information is embedded across the network and hence resistant to watermark removal attacks.

We conduct extensive evaluations on several image classification datasets (MNIST, CIFAR-10/100, and Tiny-ImageNet)

with various network architectures (LeNet-5, VGG16, and ResNet-18). The results show that our method significantly outperforms existing watermarking solutions in terms of performance and robustness.

The rest of this paper is organized as follows. We first survey related works in Section 2. Next, Section 3 defines the problem and Section 4 details the proposed solution. Experimental results are then presented in Section 5. Finally, Section 6 concludes this paper.

2 Related Work

Existing DNN watermarking methods can be divided into white-box methods and black-box methods. The white-box methods require the internal information of the DNN model for verification, while the black-box methods only need model predictions during the verification phase. We illustrate them as follows:

White-box watermarking. In this scenario, researchers inject manually selected secret information (e.g., encoded images and strings) into the model weights. Then, in the verification phase, defenders try to extract these watermarks from model weights and claim ownership of this model.

Uchida et al. [35] are the first to propose the concept of DNN watermarking. They regularize the selected weights to some secret values by adding a regularization loss during training. Li et al. [24] improve the method in [35] by adding a Spread-Transform Dither Modulation (ST-DM)-like regularization term, which can reduce the impact of watermarking on the accuracy of the DNN model on normal inputs. Chen et al. [3] improve [35] by implementing a watermarking system with anti-collision capabilities. Betty et al. [5] observe that the Adam optimiser introduces a dramatic variation in the distribution of the weights after watermarking, which can be easily detected by adversaries. Thus, the authors propose to use an orthonormal projection matrix to project the weights

and run the Adam optimizer on top of the projected weights.

Different from the scheme of Uchida’s, Tartaglione et al. [34] set the watermarked weights before the training procedures and fix them during training. Wang et al. [36] propose to embed and extract the watermark into and from the model weights via an additional independent neural network. Instead of embedding watermarks into the model weights, Rouhani et al. [30] embed the watermark into the feature maps of the DNN model. The authors first explore the Probability Density Function (PDF) of activation maps obtained in different layers, then embed the watermark in the low probabilistic regions within the model to reduce effects on clean accuracy. Considering the ambiguity attacks where attackers can disguise as a model owner to embed their watermark into the model, Fan et al. [7, 8] added a passport layer into the victim model for ownership verification and user authentication, which can resist ambiguity attacks. Guo et al. [13] first propose a series of attack strategies, such as scaling, noise embedding, and affine transformation, to fail the embedded watermarks. Then, the authors augment existing watermarks by introducing the above attack methods to watermark generation. In contrast, we develop the functional-coupled watermarks, which are conceptually different.

Black-box watermarking. This kind of watermarking method enables the verification of DNN ownership by identifying the consistency between specific inputs and the corresponding results. Such watermarks can be accomplished in terms of injecting backdoors into the model [23] or generating adversarial examples. The injected backdoor and the model’s vulnerability can be regarded as embedded watermarks, and the trigger images and adversarial examples are the corresponding keys. The backdoor-based watermarking strategies firstly generate some special samples as the backdoor trigger samples combined with the shifted labels of such images to train a backdoor model. To verify the model’s ownership, defenders can recover the watermark by querying the model and checking the consistency between outputs and the queried samples.

Adi et al. [1] use backdoors [11] for DNN watermarking. The authors conducted two different ways, including fine-tuning the models and training from scratch with the selected images as the trigger (e.g., Trigger C in Fig. 1(a)), to generate backdoors. Rouhani et al. [30] propose to retrain the model to inject backdoors as the DNN watermark for ownership verification. To generate watermarks, Zhang et al. [42] first select key images as the watermarking samples via superimposing to some of the training images a visible pattern (e.g., Trigger A & B in Fig. 1(a)). The labels of such above images are shifted to the target class, and combined with these images to train the backdoor model and build a special relationship between them as the watermarks. Considering the vulnerability under backdoor detection of visible trigger patterns, Guo et al. [12] and Li et al. [25] propose to replace the trigger pattern with the invisible ones, such as adding a bit sequence

to random pixel locations. Jia et al. [16] suggest training the features of out-of-distribution triggers (e.g., Trigger D in Fig. 1(a)) entangled with normal model features to enhance the watermarking performance in the model extraction scenario. Different from directly protecting the victim model, Szyller et al. [33] embed watermarks into the surrogate model when adversaries conduct model extraction attacks. They deploy an additional component within the API whereby the adversaries can access the model, and the API deliberately returned some wrong results corresponding to part of the input samples. In this way, the surrogate model trained by the returned information can be embedded with watermarks.

The adversarial example-based watermarking methods leverage the generated examples to shape the model boundary for building a unique connection between such dedicated samples and selected outputs. Merrer et al. [28] utilize IFGSM algorithm [10] to generate the adversarial examples as the key samples of watermarks. The contradiction between input samples and predictions can be leveraged as a special relationship to watermark the model. He et al. [15] generate sensitive-sample watermarks, aiming that small changes in model weights can be reflected in the model outputs via these sensitive samples. Yang et al. [40] propose a bi-level framework to jointly optimize adversarial examples and the DNN model. Wang et al. [37] are the first to take both robustness and transferability into consideration for generating realistic watermarks. Chen et al. [4] propose a testing framework to calculate the similarity between the victim model and the suspect model by a set of extreme test cases of adversarial examples.

3 Problem Definition

In this section, we first introduce the threat model in Section 3.1. Then, we formulate our problem in Section 3.2. Section 3.2 provides the evaluation metrics for DNN watermarking.

3.1 Threat Model

In this section, we clarify the scenario of tampering with the ownership of DNN models and watermarking the victim models. The watermarking scenario includes five subjects, including model owners, users, DNN models, community and adversaries. Specifically, the model owner designed and trained a DNN model with good performance and submitted it to the community. Users can download this model and leverage it for a downstream task. However, adversaries can also download the model and re-submit the stolen model to other communities, then claim their ownership of this model. This violates the intellectual property rights of the original owner of this DNN model. Therefore, we need a proper method to verify the ownership of the released model.

In this paper, we consider an attack scenario in that adversaries stole a model from the community, and set up an online

service to provide AI service with the leaked model. Before re-releasing the victim model, adversaries can prune it, fine-tune it with their own new data, or even add new watermarks to this model. We assume that adversaries have full access to the victim model, such as the model structure, model weights, and hyperparameters. Through pruning and fine-tuning, adversaries may erase the watermarks embedded by the real model owner; adding a new watermark enables adversaries to claim their ownership of this model. During the verification phase, we assume that the defenders can only get the prediction results of the victim model in the online service platform, yet they cannot access the internal knowledge (such as the weights) of this model. Therefore, the existing white-box DNN watermarks fail in such a scenario, and black-box methods are suitable.

3.2 Watermarking Problem Formulation

Watermarking target: Given a DNN model $f_\theta(x)$ with θ representing the model weights, a watermarking strategy $h(\cdot)$ aims to embed an abstract watermark S into the DNN model, and a recovering strategy $r(\cdot)$ aims to extract such watermarks from the candidate model.

Techniques: In terms of white-box and black-box watermarking methods, details of $h(\cdot)$ are different. White-box methods can embed and recover watermarks S from only model weights. But, black-box methods require both input samples and the model to achieve this. To this end, S is the subset of joint (x, θ) , meaning that S relies on both samples and models. The mainstream white-box methods aim to embed additional information into model weights, that is, $f_{\theta+\delta}(\cdot) = h_{white}(f_\theta(\cdot))$, with δ indicating the perturbation on model weights, and we can recover S from δ (i.e., $\delta \Rightarrow S$). In this case, apart from the selected weights, the rest of the weights in the model will not change. In contrast, with the backdoor-based black-box methods, we need to modify the whole model to embed watermarks by either fine-tuning the model or training the model from scratch with the trigger data. That is, we can generate watermarks via $\{x', f_\theta(\cdot)\} = h_{backdoor}(f_\theta(\cdot), x')$, and $(x', \theta', f_\theta(x')) \Rightarrow S$, with θ' indicating the modified model weights after injecting backdoor and x' indicating trigger samples. Generating adversarial example-based black-box watermarks is in no need of tuning the model parameters but needs to modify input data for generating adversarial examples. That is, we can generate watermarks via $\{x', f_\theta(\cdot)\} = h_{adv}(f_\theta(\cdot), x)$, and $(x', \theta, f_\theta(x')) \Rightarrow S$, with x' indicating the generated adversarial example corresponding to the input x .

During the verification phase, the recovery strategy is dedicated to extracting the watermark from the model. For white-box methods, if the decoding result of the extracted weights is in line with the watermark, i.e., $S = r(\delta)$, defenders can show their ownership of this candidate model. For black-box methods, if the prediction results of the input trigger images

or adversarial examples are consistent with the target label, i.e., $S = r(x', f_\theta(x'))$ or $S = r(x', f_\theta(x'))$, defenders can also show their ownership on this candidate model.

3.3 Evaluation Metrics

Effectiveness. The goal of effectiveness is to measure whether we can successfully verify the ownership of DNN models under the protection of the proposed watermarking method.

Fidelity. The watermark should have a limited impact on the benign accuracy of the watermarked model. That is, we should guarantee the watermarked model’s clean accuracy as close as possible to that of a model trained on the raw task.

Robustness. The robustness metric indicates the performance-preserving capability of a watermarking method under attacks. To conduct attacks, we assume that adversaries have full access to the victim model, such as the model structure, model weights, and hyperparameters. Three attacks are utilized to evaluate the robustness of a watermarking method. First, when we assume the adversaries can access the model structure, model weights, and hyper-parameters, they can prepare their own new data to **fine-tune** the given model. We select two ways to fine-tune the model, including fine-tuning with data from the original data domain and transfer learning with data from the new data domain. Generally, after fine-tuning or transferring, the weights of the victim model may shift from the original distribution, and the embedded watermarks may not work well. Second, adversaries can also **prune** the victim model to drop part of the model weights to erase the latent watermarks, since the watermark is actually a special abstract pattern in a DNN model, pruning may erase the corresponding function of the watermark. Finally, once adversaries know the underlying watermarking method, they can re-embed a new watermark to **overwrite** the existing watermark in the model to disable the recognition of original watermarks [20, 38].

4 Methodology

In this section, we present the detailed design of our new watermarking method for deep neural networks. There are three main modules, including generating triggers, embedding watermarks and watermarking verification. Our workflow is presented in Fig. 2. We first propose two alternative methods to generate feature-fusion trigger samples. Second, we use the trigger samples combined with normal data to train the watermark coupled with the fundamental model functionalities, and apply two strategies to enhance such coupling. Lastly, we present the procedures for ownership verification.

4.1 Feature-fusion Design

In this subsection, we present two kinds of feature-fusion methods, including 1) the direct feature-fusion method, and

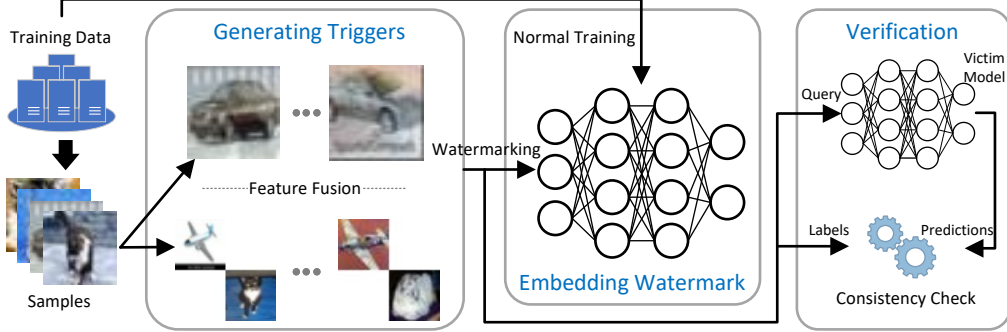


Figure 2: The workflow of the proposed function-coupled watermarking method.

2) the invisible feature-fusion method, to generate the key watermark images. Our key insight is to generate watermarks that are coupled with model functionalities. Previous trigger-pattern-based watermarking methods need to introduce out-of-distribution features (e.g., the features of trigger patterns) to the original data domain, making them difficult to evade the attacks of pruning and fine-tuning. This is because the pruning and fine-tuning are inclined to drop the information that is loosely coupled with the model functionalities. From the perspective of feature fusion, a similar technique is MixUp [41], which aims to improve the model accuracy by combining training data from different classes (a data augmentation technique). In our context, data augmentation is not our target; in contrast, we assign target labels to the combined images to use them as functional-coupled watermark triggers. To this end, we suggest fusing in-distribution features to make the watermarks coupled with the model’s normal functionalities.

4.1.1 Direct Feature-fusion Method

Suppose a dataset $X = \{X_1, X_2, \dots, X_{N_c}\}$ with N_c representing the total categories of the dataset, the watermark images are all generated based on it. Define K_{wm} as the size of the watermark image set WM . X_i and X_j are the subsets from the original dataset for selecting base instances from them to generate the watermark images, and the target class is set as $t \in [1, N_c]$ excluding i and j . Specifically, we can follow Eq. 1 to generate the watermark image set.

$$\begin{cases} WM = \{wm_1, wm_2, \dots, wm_k, \dots, wm_{K_{wm}}\} \\ L_{wm_k} = t, t \in [1, N_c] \end{cases} \quad (1a) \quad (1b)$$

where wm_k indicates each element in the watermark image set. L_{wm_k} is the corresponding given label of each generated watermark image.

Specifically, to generate a watermark image, we can combine the selected two base instances in the dimensions of height and width of the image. The watermark image has the complete features of both base instances. Suppose the shape of the base instance is (W, H, C) , we can generate the

watermark image as follows:

$$wm_k = X_i^p \oplus X_j^q \quad (2a)$$

$$wm_k^{(w,h,c)} = \begin{cases} X_i^{p,(w,h,c)}, & \text{if } w \leq W, h \leq H \\ X_j^{q,(w-W,h-H,c)}, & \text{if } w > W, h > H \\ (255, 255, 255), & \text{if } w \leq W, h > H \\ (255, 255, 255), & \text{others} \end{cases} \quad (2b)$$

where the operator \oplus means a strategy for merging two base instances from different base classes. i and j represent the two selected classes from class 1 to class N_c . p, q represent the indices of randomly selected base instances from the two base subsets (i.e., X_i and X_j), respectively.

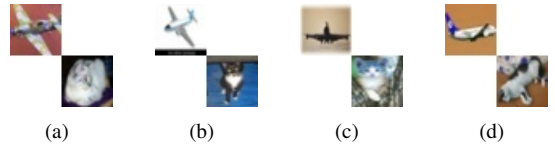


Figure 3: Examples of visible trigger images generated for Cifar-10 dataset. The top-left corners are the instances from ‘airplane’ class, and the images in the bottom-right corners are selected from the ‘cat’ class.

Pixels of each watermark image wm_k can be computed by Eq. 2b. The top-left and bottom-right corners, respectively, show the original base instances from different classes. Fig. 3 shows examples of generated watermark images. The combined images maintain all features of the base instances.

4.1.2 Invisible Feature-fusion method

The direct feature-fusion method of Eq. 2b generates a set of watermarked images in which two groups of features are independently distributed in the two corners and works well on embedding watermarks. However, adversaries can trivially detect such key samples because of the abnormal white blocks in images, which is unusual in normal images. Therefore, we use another invisible feature-fusion strategy to avoid the

auditors' visual detection. Specifically, we discard the strategy of merging features in the dimensions of width and length, but design a new method from the perspective of image depth (RGB channels).

We suppose a dataset $X = \{X_1, X_2, \dots, X_{N_c}\}$ with N_c representing the total categories to be the base for generating watermark images. X_{b1} and X_{b2} are the subsets of the original dataset for selecting instances from them to generate the watermark images. We select images from X_{b1} and X_{b2} as two sets of base instance, and the target class is set as t which is different from $b1$ and $b2$. Define K_{wm} as the size of the watermark image set WM . We can also follow Eq. 1 to generate the watermark image set. Differently, in order to generate an invisible watermark image, we need to merge the two base instances in a different way. Suppose the shape of the base instance is (W, H, C) , the watermark image can be computed as follows:

$$wm_k = X_{b1}^p \oplus X_{b2}^q \quad (3a)$$

$$wm_k^{(w,h,c)} = r \cdot X_{b1}^{p,(w,h,c)} + (1 - r) \cdot X_{b2}^{q,(w,h,c)} \quad (3b)$$

where the operator \oplus means a strategy for merging two base instances from different base classes. p, q represent the indices of randomly selected base instances from the two base subsets (i.e., X_{b1} and X_{b2}), respectively. r is a parameter (limited from 0 to 1) to change the transparency of the target instance in the merged watermark image, when increasing the value of r , the features of the target instances become more invisible (i.e., more transparent).



Figure 4: Examples of invisible trigger images generated for Cifar-10 dataset. The two base instances are selected from the 'automobile' class and the 'cat' class, respectively. The transparency ratio here is set to 0.7.

We can compute pixels of each invisible watermark image wm_k by Eq. 3b. For two source images with a shape of (W, H, C) , the merged watermark image still retains the same dimension of the original data domain. In the last step of such an invisible feature-fusion method, the labels of these merged samples are assigned as t . Fig. 4 presents examples of generated watermark images.

4.2 Masking during Training Phase

To further enhance the coupling relationship between watermarks and model functionalities, we introduce a masking training strategy during the training phase. We first formalize the training of standard backdoor-based watermarks.

4.2.1 Standard Backdoor-based Watermarking Training

We suppose a training dataset $\{(x_i, \bar{y}_i)\}_{i=1}^{N_d}$, where $X = \{x_i\}_{i=1}^{N_d}$ and $\bar{Y} = \{\bar{y}_i\}_{i=1}^{N_d}$ represent the corresponding input samples and labels, respectively, and N_d is the total number. A DNN model $f(\cdot) : X \rightarrow \bar{Y}$ is trained from the dataset to map the input samples to labels. Backdoor-based watermarking methods are typically launched by changing labels, and aim to build a surprising connection between the trigger samples and the target label. The target class is set as \bar{y}_t . Defenders can manipulate part of training samples by adding well-designed trigger patterns and change the corresponding labels to the target label, which produce a watermarking training set $\{X', Y'\} = \{(x'_i, \bar{y}_t)\}_{i=1}^{N_d \cdot e\%} + \{(x_j, \bar{y}_j)\}_{j=N_d \cdot e\% + 1}^{N_d}$, with $e\%$ denoting the ratio of the trigger data. Defenders then can exploit the manipulated dataset to train the model, producing a watermarking model $f_{wm}(\cdot)$.

4.2.2 Masking Training Strategy

Different from the standard backdoor-based watermarking, sparsely training a network with random masks in the training phase can improve the robustness of models against attacks. A similar technique that can be leveraged to make the network sparse is Dropout [32]. It is a prevailing method introduced during the model training phase to improve the generalization ability of the model. Dropout is usually applied in the fully-connected hidden layers [9]. In contrast, we propose a masking training strategy and apply it to the convolutional layers of DNN models. Our key insight is to equally distribute the watermark function to each neuron by iteratively randomly masking and training, which disables attacks that are conducted by dropping key neurons.

Proposition: introducing the sparse training method to the convolutional layers can reduce the negative impacts brought by pruning/fine-tuning in the future verification phase.

Proof: A masking strategy can disable part of neurons' updating in the training phase. We can iteratively add random masks during training to avoid model performance relying heavily on a small number of critical neurons. Such neuron weights may be dropped or heavily shifted after pruning/fine-tuning, causing a fatal degradation of model accuracy or watermarking performance. In contrast, through randomly masking we can distribute watermark functions to each neuron equally, thus different combinations of neurons have the potential to retain the full watermark function. Therefore, we adopt such a masking strategy to enhance watermarking robustness.

Two keys to masking methods during the training phase are 1) masking strategies and 2) masking ratios. We need to control the weights updating in order to introduce the sparsity into both the convolutional and full-connected layers. Since the manipulation occurs in the training phase, we need not only to apply the sparse strategy during the forward prop-

agation, but also to freeze the selected weights during the backward updating. To this end, a feasible way is to randomly mask part of the weights of DNN layers. Such a mask also mimics the operations of pruning operations conducted by adversaries. We can apply different masks to mimic various pruning principles (such as global pruning and module-based pruning) referring to Eq. 4. To ensure that the masking training strategy is general to different pruning attacks, in practice, we only adopt random masks to train the watermarked model.

Sparse mask:

$$\begin{cases} y = f(((W \odot M)/(1-p))x + b), \\ M_{i,j} \sim \text{Prune}(\{\text{random, global, module, } \dots\}, p) \end{cases} \quad (4)$$

Inference phase:

$$y = f(Wx + b) \quad (5)$$

where $f(\cdot)$ indicates the DNN model for training and testing. W, x, b represent the weights, inputs, and biases, respectively. We use $0 \leq p \leq 1$ to indicate the ratio of the preserved elements after masking. M is the mask that is used to indicate the pruned part of the convolutional kernels, and M corresponds to the pruning strategy chosen in the inference phase, i, j indicate the position of these kernels. The operator \odot is the element-wise multiplication. Prune means the pruning strategies that depend on the parameters including the specific pruning principle (such as global pruning and module-based pruning) and the pruning ratio. To ensure the same expectation as the original outputs, the calculation results need to be scaled by multiplying with $1/(1-p)$.

Then, we can update the model weights as follows:

$$W' = W - \eta \cdot \left(\frac{\partial L}{\partial W} \odot M \right) / (1-p) \quad (6)$$

where W' is the temporary variable of neural network weights, η is the learning rate and controls the gradient updating step size, L represents the model loss.

Different from the normal gradient updating method, we mask the updating gradients with M and then apply them to the weights. For each iteration, the gradient updating operation is only worked on the weights that are preserved after masking with M .

4.3 Fine-tuning during Training Phase

Fine-tuning is a common method to weaken the performance of the DNN watermark, since it can make the model preserve the knowledge learned from the new data domain but drop the knowledge learned from some specially designed data. We mimic the fine-tuning operation to design a similar strategy when training a model to enhance the watermarking robustness under fine-tuning attacks.

Proposition: introducing a fine-tuning-like strategy to the training phase can reduce the negative impacts on watermarks brought by fine-tuning in the verification phase.

Proof: there are two keys to the training-time fine-tuning strategy, i.e., learning rate and the fine-tuning data. Fine-tuning has a smaller learning rate than training from scratch, since a large learning rate applied in the fine-tuning process can bring a negative impact on the performance of the extractor. Differently, training from scratch initializes a large learning rate and then reduces it to a smaller one with the number of iterations. Therefore, similar to the adversarial training method to defend against adversarial example attacks, applying the fine-tuning strategy with small learning rates to the training phase allows the model to adapt to the effects of fine-tuning in advance.

We consider two different attack scenarios, including fine-tuning with data that is independently identical distribution with the training data and transfer learning with data from other datasets. However, the out-of-distribution data is usually unavailable and uncontrollable when training the watermark model, we can only use the data from the original dataset. To this end, we use the data from the independently identical distribution with the training data in a **small learning rate** to ‘fine-tune’ the model during the training phase. Therefore, ‘fine-tune’ is an additional operation between batches or between epochs, and it can be formalized as follows:

$$W' = W - \eta' \cdot \left(\frac{\partial L_{\text{finetune}}}{\partial W} \odot M \right) / (1-p) \quad (7)$$

where W and W' are the weights and temporary variables of neural network weights, respectively. η' is the learning rate and controls the gradient updating step size for the fine-tuning operation during the training phase. L_{finetune} represents the model loss calculated on ‘fine-tune’ data.

Suppose the fine-tuning dataset is $\{X_{ft}, \bar{Y}_{ft}\}$ with K_{ft} samples, we can calculate the loss value of the model on such fine-tuning data by Eq. 8.

$$L_{\text{finetune}} = \frac{1}{K_{ft}} \cdot \sum_{i=1}^{K_{ft}} CE(f(x_{ft}^i), \bar{y}_{ft}^i) \quad (8)$$

where $CE(\cdot)$ calculates the cross entropy between predictions and ground-truth labels, $\{x_{ft}^i, \bar{y}_{ft}^i\}$ is a sample of the fine-tuning dataset.

Combining all the operations for generating watermarks and improving the watermarking robustness, the overall watermarking procedures are formalized as Algorithm 1.

4.4 Procedures of Ownership Verification

In black-box watermarking scenarios, we send queries to the remote AI service with previously generated watermarking samples to verify the ownership of the candidate model. If the response matches the expected labels, we can confirm that the

Algorithm 1 Procedures for watermarking.

Input: L -layer initialize model $f(\cdot)$ with N_c classes, training dataset X , watermark image set WM with the size of K_{wm} , weight mask M , fine-tuning data X_{ft} with size of K_{ft} , training epochs $EPOCHS$, batch size $BatchSize$, learning rate η for normal training data and learning rate η' for fine-tuning data.

Output: A watermarking model robust to fine-tuning and pruning.

/* Step 1: preparing watermarking data */

- 1: Generate watermarking data WM by Eq. 2 or Eq. 3

$$WM = \{wm_1, wm_2, \dots, wm_k, \dots, wm_{K_{wm}}\}$$

$$L_{wm_k} = t, t \in [1, N_c]$$

/* Step 2: preparing fine-tuning data */

- 2: Select fine-tuning data X_{ft} from the independently identical distribution with the training data.

/* Step 3: training phase */

- 3: **for** epoch in $EPOCHS$ **do**
 - // Training on normal data
 - 4: initialize weight mask M .
 - 5: Set optimization target: $\min_W L(f(W, X), Y)$
 - 6: **for** iter in $BatchSize$ **do**
 - 7: Calculate predictions via:
 $y = f(((W \odot M) / (1 - p)) \cdot x + b)$
 - 8: Update weights via:
 $W' = W - \eta \cdot (\frac{\partial L}{\partial W} \odot M) / (1 - p)$
 - 9: **end for**
 - // Training on fine-tuning data
 - 10: Calculate loss value on fine-tuning data via:
 $L_{finetune} = \frac{1}{K_{ft}} \cdot \sum_{i=1}^{K_{ft}} CE(f(x_{ft}^i), \bar{y}_{ft}^i)$
 - 11: Update weights via:
 $W' = W - \eta' \cdot (\frac{\partial L_{finetune}}{\partial W} \odot M) / (1 - p)$
 - 12: **end for**

remote AI service is powered by our protected model. This is because DNN models without embedding watermarks will not have the capability to correctly recognize the given key samples, and such queries will generate wrong predictions. In fact, the probability that a DNN model misclassifies all the watermark samples to the same pre-defined label is extremely low, causing a low false-positive rate. For ownership verification, defenders can first submit a set of prepared watermark samples (e.g., with a number of 90) to the remote AI service platform. Then, they need to collect the corresponding predictions of these queries. Since each key sample is equipped with the target label, defenders can calculate the authentication success rate with their labels and the collected predictions. If the authentication success rate is higher than a widely accepted threshold by the community, defenders can claim their ownership of this victim model.

5 Experimental Results

In this section, we present the experimental results of the proposed watermarking method. The following parts of this section are organized as follows. In Section 5.1, we leverage different network structures and datasets to train DNN models as the victims, and present their accuracy on the clean dataset. In Section 5.2, we present the watermarking performance of different models and the watermarking impact on benign accuracy. In Section 5.3, we evaluate the robustness of the proposed method under three prevailing attacks. Finally, in section 5.4, we compare the proposed method with six state-of-the-art watermarking methods.

5.1 Experimental Settings

We evaluate our feature-fusion watermarking method on several common networks and datasets, including LeNet-5 [18], VGG16 [31], and ResNet-18 [14] models on, MNIST, CIFAR-10 [17], CIFAR-100 and Tiny-ImageNet (200 classes) [39]. Table 1 presents the benign accuracy on these trained models. We adopt two feature-fusion methods (examples can refer to Fig. 3 and Fig. 4) to generate watermarks. For each experiment, we set less than 1% of the training data as the watermarking samples, and fix the number of validation images to 90. Three transparency rates (r) of 0.5, 0.7, and 0.9 are set to generate invisible feature-fusion triggers. For ease to conduct experiments, we set $r = 0.5$ in Section 5.3 and Section 5.4 to evaluate the robustness, and compare with other methods.

Table 1: Benign accuracy of different models.

Models	Classes	Top-1 Benign accuracy (mean)
MNIST (LeNet5)	10	99.14%
CIFAR-10 (ResNet-18)	10	94.49%
CIFAR-100 (VGG16)	100	73.13%
Tiny-ImageNet (ResNet-18)	200	65.98%

In addition to using models without watermarks as the baseline, we also perform empirical evaluations of our proposed feature-fusion watermarking method against five other black-box approaches:

- Backdoor-based methods: Protecting IP [42], Turning weakness into strength [1], Exponential weighting [29], and Entangled watermark [16].
- Adversarial example-based method: Frontier stitching [28].

5.2 Effectiveness and Fidelity

The metric of effectiveness is to measure whether we can successfully verify the ownership of DNN models with our watermarking method. The watermarking operation should have

Table 2: Results on effectiveness and fidelity.

Methods	Hyper-parameter changing	MNIST (LeNet5)		CIFAR-10 (ResNet-18)		CIFAR-100 (VGG16)		Tiny-ImageNet (ResNet-18)	
		Eff.	Fid.	Eff.	Fid.	Eff.	Fid.	Eff.	Fid.
Direct	#1	100%	99.13%	100%	94.95%	100%	73.17%	100%	65.44%
	#2	100%	99.14%	100%	94.94%	100%	73.17%	100%	65.42%
	#3	100%	99.13%	100%	94.94%	100%	73.16%	100%	65.43%
Invisible	r=0.5	100%	99.12%	100%	94.15%	100%	72.92%	100%	65.49%
	r=0.7	100%	99.11%	100%	94.16%	100%	72.89%	100%	65.48%
	r=0.9	100%	99.13%	100%	94.14%	100%	72.91%	100%	65.45%

a limited impact on the clean accuracy of the watermarked model, i.e., the watermarked model should guarantee its clean accuracy as close as possible to that of a model trained on the same dataset without embedding watermarks. We evaluate the proposed two methods on four different models in terms of effectiveness and fidelity. Each method has three sets of experiments. For the direct feature-fusion method, three replicate experiments are performed (numbered #1, #2, and #3). For the invisible feature-fusion method, we change the transparency ratio from $r = 0.5$ to $r = 0.9$.

Table 2 presents the proposed methods' effectiveness and fidelity. In all these experiments, the verification effectiveness of the two proposed methods all achieves the level of 100%, which indicates the watermarking methods are effective. Referring to the baseline of benign accuracy listed in Table 1, the generated watermarked models can achieve a high watermarking success rate without sacrificing clean accuracy. Specifically, the perturbation of the proposed watermarking methods on the benign accuracy of the model is within the range of $\pm 0.5\%$. Most of the experiments show a small decrease in benign accuracy. The accuracy of CIFAR-10 models even increases from the level of 94.4% to the level of 94.9% after watermarking. We think this result is isolated and accidental since the benign accuracy decreases slightly in most cases. Three replicate experiments for each method show similar performance in terms of both effectiveness and fidelity. For the invisible feature-fusion method, the watermarking performance under three different transparency ratios is also very close to each other. This phenomenon indicates that transparency has little effect on the final watermarking performance, and it only affects the visual features.

5.3 Robustness

Fine-tuning resistance. In order to conduct the fine-tuning attack, we select a small number of in-distribution samples as fine-tuning data. The amount of fine-tuning data fluctuates between 1000 and 2000 according to the size of the dataset. We also evaluate the robustness metric under different fine-tuning trials (from 1 to 10). Fig. 5 and Fig. 6 present the watermarking performance under fine-tuning attacks. The experimental results show that both feature-fusion methods perform well against fine-tuning attacks.

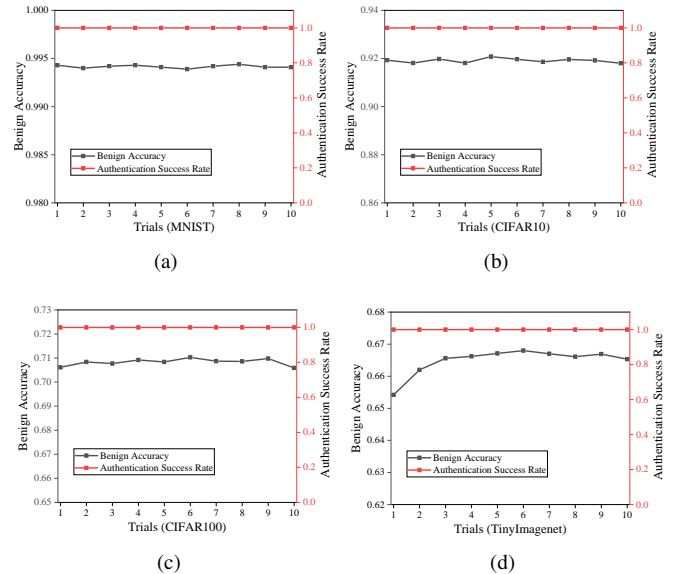


Figure 5: Fine-tuning results of direct watermarking on benign accuracy and authentication success rate.

Fig. 5 presents the experimental results of the direct feature-fusion watermarking method. The authentication success rate stabilizes at 100% as the number of training trials increase, and the benign accuracy of several models (MNIST, CIFAR-10, and CIFAR-100) fluctuate slightly. The benign accuracy of the model trained on Tiny-ImageNet even shows a slight upward trend from trial #1 to #6. A reasonable explanation is that the model learned new critical features after fine-tuning, which can improve the model's performance. Fig. 6 shows the experimental results of the invisible feature-fusion watermarking method. Similar observations indicate that this method is also robust to fine-tuning attacks.

We also conduct experiments to verify watermarking robustness in transfer learning scenarios. In detail, we conduct three groups of transfer learning tasks, including CIFAR-10 to CIFAR-100, CIFAR-10 to MNIST and CIFAR-100 to Tiny-ImageNet. For each group of experiments, we change the datasets but retain the number of classes, and the learning rate is set to 1e-4. For example, we randomly select 10 classes

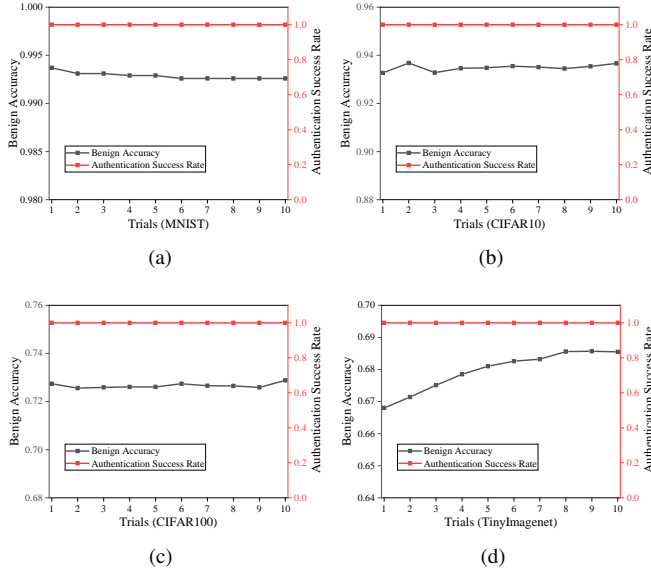


Figure 6: Fine-tuning results of invisible watermarking on benign accuracy and authentication success rate.

from CIFAR-100 to complete the transfer learning from the CIFAR-10 dataset. Fig. 7 presents the authentication success rate and accuracy on the original dataset for each group of transfer learning tasks. The results show that transfer learning affects both the authentication success rate and the model’s accuracy on the original dataset, but the authentication success rate of these three groups is still above 70% after 10 trials of transfer learning. In contrast, transfer learning affects the model’s accuracy on the original datasets more, especially in the transfer learning tasks of CIFAR-10 to MNIST and CIFAR-100 to Tiny-ImageNet. After transfer learning for the two tasks, the accuracy on the original datasets even decreases by under 20%. A reasonable explanation is that the target data domain is very different from the original one in these two tasks, but CIFAR-10 and CIFAR-100 are similar to each other.

Weight pruning resistance. In order to evaluate our method against the pruning attack, we adopt the L1-norm unstructured pruning strategy which is widely used in prior work. It means determining whether the parameters should be pruned based on the values of the weights. The pruning ratios are set from 0.1 to 0.9, meaning the rate of the pruned weights ranges from 10% to 90%. Fig. 8 and Fig. 9 present the watermarking performance under pruning attacks. The experimental results show that both feature-fusion methods perform well against the pruning attacks on the four models.

As shown in Fig. 8, the experimental results of the direct feature-fusion watermarking method against the pruning attack are presented. The results show our method still works well when the pruning rate is set to be greater than 0.7. Since pruning model weights can affect the benign accuracy of the model, the pruning ratio is actually a trade-off between model

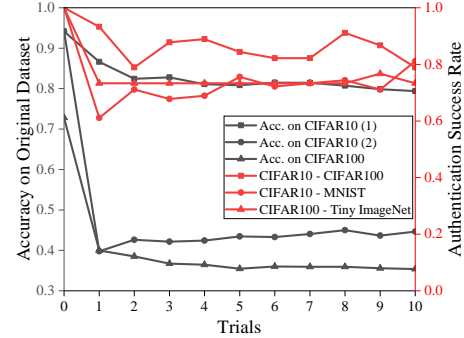
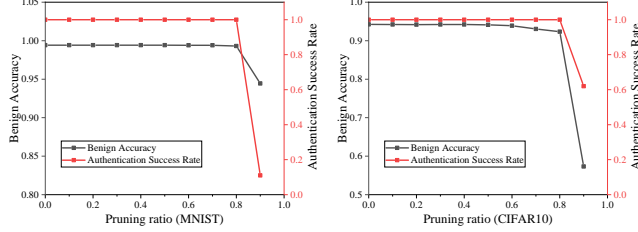


Figure 7: Watermarking robustness under transfer learning. Acc. on CIFAR10(1) represents the model accuracy on the CIFAR-10 dataset after the transfer learning of CIFAR-10 to CIFAR-100. Acc. on CIFAR10(2) represents the model accuracy on the CIFAR-10 dataset after the transfer learning of CIFAR-10 to MNIST.

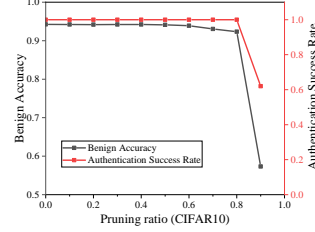
sparsity and model accuracy. As the pruning ratio increase, our watermarking success rate is still high when the model is not available in terms of clean accuracy. The watermarks embedded into the MNIST model and CIFAR-10 model perform well till the pruning ratio is set to greater than 0.8. The benign accuracy of both above models also decrease dramatically when the pruning ratio is set to 0.9. Differently, the authentication success rate of the watermark on the CIFAR-100 model is consistently at 100% with the increase of the pruning ratio from 0.1 to 0.9. But its benign accuracy dramatically decreases when the pruning ratio is greater than 0.6. In addition, the watermark on the Tiny-ImageNet model can work stably when the pruning ratio is less than or equal to 0.7. However, the pruning attack has a greater negative impact on the benign accuracy of the model.

The above experiments show that watermarks are more robust under pruning attacks than the basic classification function (clean accuracy) of the model. This is because the capacity of the model becomes small as the pruning ratio increases. Meanwhile, watermarking requires much less model capacity than the basic classification function of such a model. Pruning has a greater impact on the classification accuracy of the model than the watermarking performance. Therefore, our watermarking method performs well on a variety of models. Compared with the small-scale datasets and models, the proposed method is more sensitive to the pruning attack when the dataset is larger. A reasonable explanation is that this phenomenon is also related to the capacity of the model, i.e., the model trained on a small-scale dataset has more unimportant parameters compared with that trained on a large-scale dataset. Fig. 9 shows the experimental results of the invisible feature-fusion watermarking method against pruning attacks. Similar phenomena can also be observed in these experiments compared with that of the direct watermarking strategy.

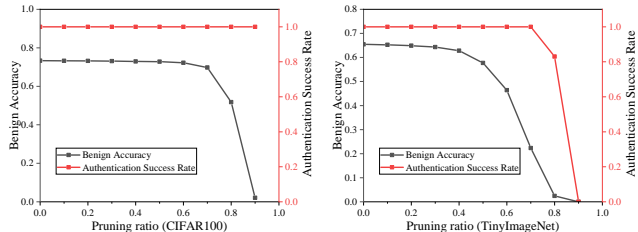
Overwriting resistance. In the watermark overwriting



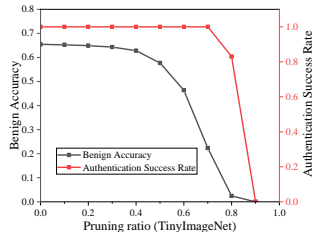
(a)



(b)



(c)



(d)

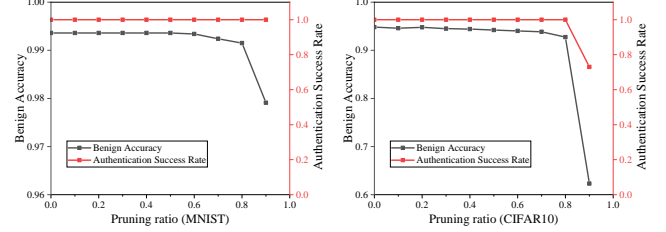
Figure 8: Pruning results of direct watermarking on benign accuracy and authentication success rate.

scenario, adversaries seek to insert new watermarks into the model in order to disable the recognition of original watermarks. We evaluate our method’s robustness under overwriting attacks by setting a similar watermarking strategy but changing the watermark samples, source classes and target class. In this case, we set No.0 and No.3 to be the source classes and No.1 to be the target class in the test group when conducting CIFAR-10 experiments. In the control group, we transfer the source classes to No. 2 and No.4 and select No. 5 as the target class. To overwrite another watermark into the model, we fine-tune the watermarked models with the selected watermark samples in a small learning rate of 1e-4. We follow this strategy to construct several pairs of experiments for various datasets and watermarking strategies. The experimental results are shown in Table 3 and the last column of Table 4.

Table 3: Overwriting results of watermarking methods on authentication success rate.

Datasets	MNIST		CIFAR-10		CIFAR-100		Tiny-ImageNet	
Source Class ID	No.2	No.4	No.2	No.4	No.9	No.13	No.9	No.13
Target Class ID	No.5		No.5		No.16		No.16	
Strategies	Direct	100%	100%	100%	100%	100%	100%	100%
New Watermarks	100%		100%		100%		100%	

As shown in Table 3, our method shows a good robust performance against overwriting attacks. After overwriting a new watermark with the same strategy, both feature-fusion watermarking methods still have a 100% accuracy on authentication success rate. This is because the process of overwriting



(a)

(b)

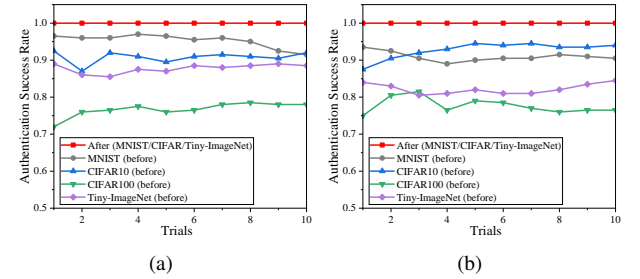
(c)

(d)

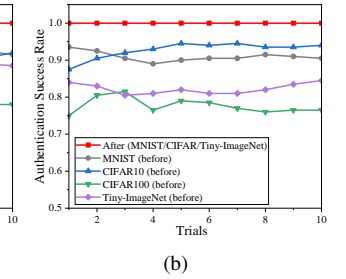
Figure 9: Pruning results of invisible watermarking on benign accuracy and authentication success rate.

is similar to that of fine-tuning and transfer learning, the difference is the type of training data. Compare with the above two attacks, overwriting even has a smaller changing impact on the watermarked model due to the training data scale. Our methods show their robustness against the above two attacks, thus it is reasonable to see the robust results under overwriting attacks. Note that the authentication success rate of the new embedded watermarks is also 100%. This is because our watermarking methods mainly focus on improving the robustness of watermarks under overwriting, but cannot prevent embedding new watermarks in the same model.

We also conduct several additional experiments to explore the impact on the robustness capability after equipping masking training and training-time fine-tuning strategies.



(a)



(b)

Figure 10: Comparison of watermarking robustness on fine-tuning attacks before and after equipping robustness-enhancing strategies.

Fig. 10 shows the difference in watermarking robustness on fine-tuning attacks before and after equipping enhancing

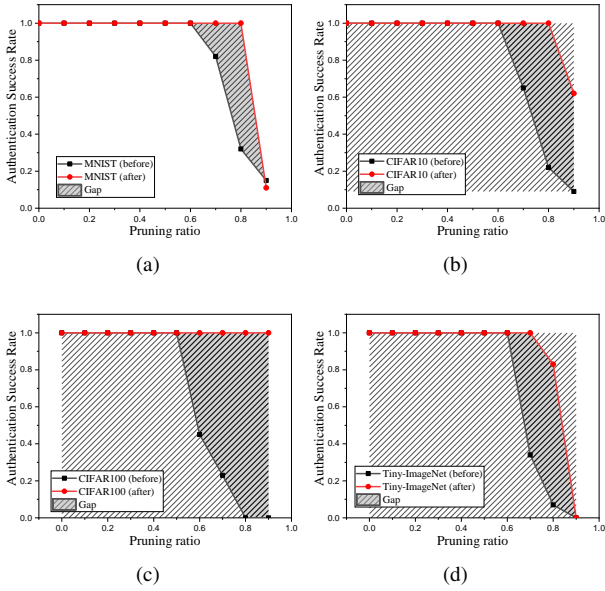


Figure 11: The effect of enhancing strategy on the robustness of direct feature-fusion method.

strategies. In these two figures, the red lines and other colored lines represent the watermarking authentication success rate of each model after and before equipping the enhancing strategies. It is clear that leveraging the mask training and training-time fine-tuning strategies can improve the watermarking robustness against fine-tuning attacks. We get an average of 10% increase on the four tasks after equipping such an enhancing strategy. The authentication success rate even increases by more than 20% on CIFAR-100 models after equipping the robustness-enhancing strategy.

Fig. 11 and Fig. 12 show the change of watermarking robustness under pruning attacks before and after equipping enhancing strategies. The watermarking authentication success rate of each model after equipping the enhancing strategies is represented with red lines, otherwise the black lines. We can observe an obvious improvement in the authentication success rate by equipping two enhancing methods, especially when the pruning ratio is set larger than 70%. For the Tiny-ImageNet dataset in Fig. 11, when the pruning ratio is set to 80%, the authentication success rate is less than 10% before applying the proposed strategy but becomes around 80% after equipping the enhancing method. This is because the feature-fusion and random masking strategy can force the model to learn to couple the watermark with model functionalities and equally distribute the watermark functions to each neuron in the model. Pruning a large percentage of neurons may disable the watermark, but also reduce the clean accuracy making the model unusable.

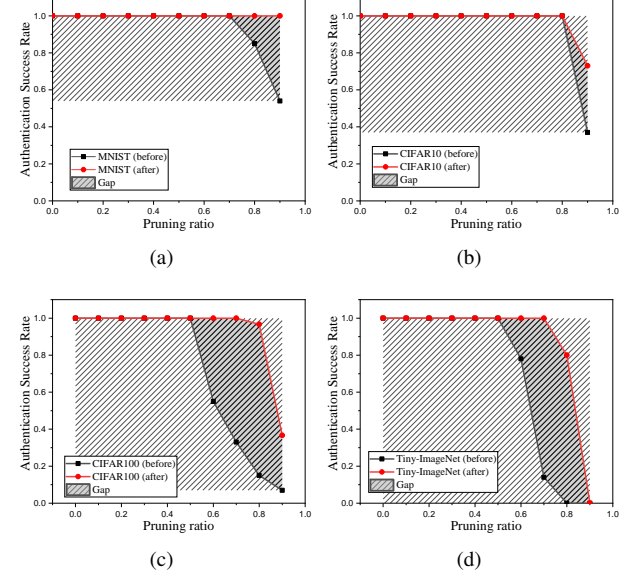


Figure 12: The effect of enhancing strategy on the robustness of invisible feature-fusion method.

5.4 Comparison with Baselines

We compare the performance of our method with state-of-the-art methods, including Protecting IP [42], Turning weakness into strength [1], Exponential weighting [29], Frontier stitching [28], and Entangled watermark [16]. Note that, since Entangled watermark focuses on the model extraction attack, and two main subjects (the victim model and the extracted model) are included in this scenario, we compare the watermarked model guided by our methods with both models. The experiments are conducted from the perspective of the authentication success rate, benign accuracy preserving rate, and robustness under four different attacks. Since the released codes of most of the works we compared are constructed based on CIFAR-10, we chose the same dataset as the benchmark for comparison. All the other methods are implemented based on the released open-source codes from GitHub ¹.

Table 4 shows the summarized experimental results. In 10-trials fine-tuning and transfer learning, the average authentication success rate of our methods outperforms that of most of the other black-box methods by 15% and 10%, respectively. We also conduct a detailed case study for such two attack scenarios, and the results are shown in Fig. 13, and Fig. 14. After pruning 80% of neuron weights, our methods still remain an authentication success rate of 100%, and the degradation of clean accuracy is lower than 1%. In contrast, the best authentication success rate of other methods is lower than 90% and degradation of clean accuracy is larger than 10% on average,

¹We conducted experiments of Ref. [1, 28, 29, 42] referring to <https://github.com/mathebell/model-watermarking>, and Ref. [16] referring to <https://github.com/RorschachChen/entangled-watermark-torch>

Table 4: Comparison with state-of-the-art methods.

Methods	Authentication success rate	Benign accuracy preserving rate	Robustness			
			Fine-tuning	Transfer learning	Pruning	Overwriting
Protecting IP [42]	100.0%	99.95%	89.00%	70.0%	89.32%	85.10%
Turning weakness into strength [1]	100.0%	99.85%	84.21%	41.0%	74.56%	82.00%
Exponential weighting [29]	100.0%	99.92%	82.00%	38.0%	83.75%	83.30%
Frontier stitching [28]	100.0%	99.90%	43.10%	30.0%	83.62%	68.40%
Entangled-victim [16]	87.41%	98.76%	95.98%	63.73%	41.71%	-
Entangled-extract [16]	75.43%	85.23%	16.14%	8.89%	58.22%	-
Ours (direct)	100.0%	99.86%	100.0%	78.20%	100.0%	100.0%
Ours (invisible)	100.0%	99.93%	100.0%	78.90%	100.0%	100.0%

which leads models to fail in normal functions.

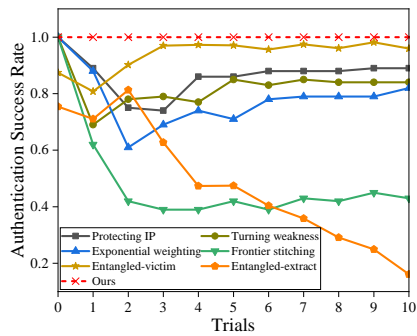


Figure 13: Fine-tuning results on authentication success rate.

As shown in Fig. 13, our methods have a significant superiority of robustness against fine-tuning attacks compared with other methods. Specifically, our watermarking methods retain an authentication success rate of 100% in 10 trials of fine-tuning, while most of the other methods can only keep around 80% of their original performance. Fine-tuning attacks affect Frontier Stitching [28] more, and its authentication success rate decreases to only around 40% after fine-tuning. We can also observe that although the initial authentication success rate of Entangled-victim is only around 87%, as the number of fine-tuning trials increases, it can achieve higher than 95%. The entangled training strategy for watermarking may play an important role to achieve this. The watermark features are entangled with that corresponding to the normal functions of a model, thus fine-tuning with in-distribution data cannot drop watermarks but even improve the watermarking performance. However, the Entangled watermark samples are beyond the training data distribution, and may degrade watermarking performance after transfer learning with out-of-distribution data. The following experimental results confirmed this hypothesis.

We also compare our method with several black-box methods in terms of watermarking robustness under transfer learning attacks. To maintain consistency in standards, we conduct transfer learning experiments from the CIFAR-10 dataset to the CIFAR-100 dataset, and the learning rate is also fixed to

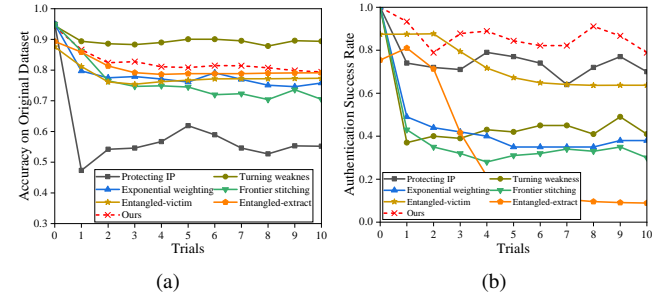


Figure 14: Watermarking robustness of different methods under transfer learning from CIFAR-10 to CIFAR-100. (a) Clean accuracy. (b) Authentication success rate.

1e-4. Fig. 14 presents the comparison results. Our method outperforms other methods obviously in preserving the watermark’s authentication success rate. Specifically, the authentication success rate of our method after transfer learning is averagely 10% higher than that of the best among other black-box methods, even around 60% higher than that of Frontier Stitching. An interesting observation is that our method performs well in preserving both clean accuracy and authentication success rate, while other methods can only perform well on one side. A possible reason is that the weights of the model trained with our method shift less than that trained with other methods after transfer learning.

6 Conclusion and Future Work

In this paper, we propose a novel black-box watermarking method to protect deep neural network models. We first introduce the concept of function-coupled watermarks that tightly integrate the watermark information with the DNN model functionalities. Based on this concept, our designed watermark triggers only employ features learnt from in-distribution data and thus do not suffer from oblivion with model retraining. To further enhance the robustness under watermark removal attacks, we apply random masking when training wa-

termarked models. Experiments conducted on various image classification tasks show that our method significantly outperforms existing watermarking methods.

In our opinion, the proposed function-coupled watermarking concept for DNN IP protection is simple yet general, despite being verified only on image classification tasks. We plan to extend it to other deep learning tasks, e.g., object detection and speech recognition.

References

- [1] Yossi Adi, Carsten Baum, Moustapha Cissé, Benny Pinkas, and Joseph Keshet. Turning your weakness into a strength: Watermarking deep neural networks by backdooring. In *Proc. of USENIX Security*, pages 1615–1631, 2018.
- [2] Arpit Bansal, Ping-Yeh Chiang, Michael J. Curry, Rajaiv Jain, Curtis Wigington, Varun Manjunatha, John P. Dickerson, and Tom Goldstein. Certified neural network watermarks with randomized smoothing. In *Proc. of ICML*, pages 1450–1465, 2022.
- [3] Huili Chen, Bita Darvish Rouhani, Cheng Fu, Jishen Zhao, and Farinaz Koushanfar. Deepmarks: A secure fingerprinting framework for digital rights management of deep learning models. In *Proc. of ICMR*, pages 105–113, 2019.
- [4] Jialuo Chen, Jingyi Wang, Tinglan Peng, Youcheng Sun, Peng Cheng, Shouling Ji, Xingjun Ma, Bo Li, and Dawn Song. Copy, right? A testing framework for copyright protection of deep learning models. In *Proc. of SP*, pages 824–841, 2022.
- [5] Betty Cortiñas-Lorenzo and Fernando Pérez-González. Adam and the ants: On the influence of the optimization algorithm on the detectability of dnn watermarks. *Entropy*, 22(12):1379, 2020.
- [6] Joachim J. Eggers and Bernd Girod. Blind watermarking applied to image authentication. In *Proc. of ICASSP*, pages 1977–1980, 2001.
- [7] Lixin Fan, Kam Woh Ng, Chee Seng Chan, and Qiang Yang. Deepipr: Deep neural network ownership verification with passports. *IEEE Transactions on Pattern Analysis and Machine Intelligence*, 44(10):6122–6139, 2022.
- [8] Lixin Fan, KamWoh Ng, and Chee Seng Chan. Rethinking deep neural network ownership verification: Embedding passports to defeat ambiguity attacks. In *Proc. of NeurIPS*, pages 4716–4725, 2019.
- [9] Golnaz Ghiasi, Tsung-Yi Lin, and Quoc V. Le. Dropblock: A regularization method for convolutional networks. In *Proc. of NeurIPS*, pages 10750–10760, 2018.
- [10] Ian J. Goodfellow, Jonathon Shlens, and Christian Szegedy. Explaining and harnessing adversarial examples. In *Proc. of ICLR*, 2015.
- [11] Tianyu Gu, Kang Liu, Brendan Dolan-Gavitt, and Siddharth Garg. Badnets: Evaluating backdooring attacks on deep neural networks. *IEEE Access*, 7:47230–47244, 2019.
- [12] Jia Guo and Miodrag Potkonjak. Watermarking deep neural networks for embedded systems. In *Proc. of ICCAD*, page 133, 2018.
- [13] Shangwei Guo, Tianwei Zhang, Han Qiu, Yi Zeng, Tao Xiang, and Yang Liu. Fine-tuning is not enough: A simple yet effective watermark removal attack for DNN models. In *Proc. of IJCAI*, pages 3635–3641, 2021.
- [14] Kaiming He, Xiangyu Zhang, Shaoqing Ren, and Jian Sun. Deep residual learning for image recognition. In *Proc. of CVPR*, pages 770–778, 2016.
- [15] Zecheng He, Tianwei Zhang, and Ruby Lee. Sensitive-sample fingerprinting of deep neural networks. In *Proc. of CVPR*, pages 4729–4737, 2019.
- [16] Hengrui Jia, Christopher A. Choquette-Choo, Varun Chandrasekaran, and Nicolas Papernot. Entangled watermarks as a defense against model extraction. In *Proc. of USENIX Security*, pages 1937–1954, 2021.
- [17] Alex Krizhevsky, Geoffrey Hinton, et al. Learning multiple layers of features from tiny images. *Technical Report*, 2009.
- [18] Yann LeCun, Léon Bottou, Yoshua Bengio, and Patrick Haffner. Gradient-based learning applied to document recognition. *Proceedings of the IEEE*, 86(11):2278–2324, 1998.
- [19] Fang-Qi Li, Shi-Lin Wang, and Yun Zhu. Fostering the robustness of white-box deep neural network watermarks by neuron alignment. In *Proc. of ICASSP*, pages 3049–3053, 2022.
- [20] Huiying Li, Emily Wenger, Shawn Shan, Ben Y. Zhao, and Haitao Zheng. Piracy resistant watermarks for deep neural networks. *arxiv:1910.01226*, 2019.
- [21] Meng Li, Qi Zhong, Leo Yu Zhang, Yajuan Du, Jun Zhang, and Yong Xiangt. Protecting the intellectual property of deep neural networks with watermarking: The frequency domain approach. In *Proc. of TrustCom*, pages 402–409, 2020.

[22] Shen Li, Yanli Zhao, Rohan Varma, Omkar Salpekar, Pieter Noordhuis, Teng Li, Adam Paszke, Jeff Smith, Brian Vaughan, Pritam Damania, and Soumith Chintala. Pytorch distributed: Experiences on accelerating data parallel training. *Proceedings of the VLDB Endowment*, 13(12):3005–3018, 2020.

[23] Yiming Li, Yong Jiang, Zhifeng Li, and Shu-Tao Xia. Backdoor learning: A survey. *IEEE Transactions on Neural Networks and Learning Systems (Early Access)*, pages 1–18, 2022.

[24] Yue Li, Benedetta Tondi, and Mauro Barni. Spread-transform dither modulation watermarking of deep neural network. *Journal of Information Security and Applications*, 63:103004, 2021.

[25] Zheng Li, Chengyu Hu, Yang Zhang, and Shanqing Guo. How to prove your model belongs to you: A blind-watermark based framework to protect intellectual property of dnn. In *Proc. of ACSAC*, pages 126–137, 2019.

[26] Hanwen Liu, Zhenyu Weng, and Yuesheng Zhu. Watermarking deep neural networks with greedy residuals. In *Proc. of ICML*, pages 6978–6988, 2021.

[27] Nils Lukas, Yuxuan Zhang, and Florian Kerschbaum. Deep neural network fingerprinting by conferrable adversarial examples. In *Proc. of ICLR*, 2021.

[28] Erwan Le Merrer, Patrick Pérez, and Gilles Trédan. Adversarial frontier stitching for remote neural network watermarking. *Neural Computing and Applications*, 32(13):9233–9244, 2020.

[29] Ryota Namba and Jun Sakuma. Robust watermarking of neural network with exponential weighting. In *Proc. of AsiaCCS*, pages 228–240, 2019.

[30] Bita Darvish Rouhani, Huili Chen, and Farinaz Koushanfar. Deepsigns: An end-to-end watermarking framework for ownership protection of deep neural networks. In *Proc. of ASPLOS*, pages 485–497, 2019.

[31] Karen Simonyan and Andrew Zisserman. Very deep convolutional networks for large-scale image recognition. In *Proc. of ICLR*, 2015.

[32] Nitish Srivastava, Geoffrey E. Hinton, Alex Krizhevsky, Ilya Sutskever, and Ruslan Salakhutdinov. Dropout: a simple way to prevent neural networks from overfitting. *Journal of Machine Learning Research*, 15(1):1929–1958, 2014.

[33] Sebastian Szyller, Buse Gul Atli, Samuel Marchal, and N. Asokan. DAWN: dynamic adversarial watermarking of neural networks. In *Proc. of MM*, pages 4417–4425, 2021.

[34] Enzo Tartaglione, Marco Grangetto, Davide Cavagnino, and Marco Botta. Delving in the loss landscape to embed robust watermarks into neural networks. In *Proc. of ICPR*, pages 1243–1250, 2020.

[35] Yusuke Uchida, Yuki Nagai, Shigeyuki Sakazawa, and Shin’ichi Satoh. Embedding watermarks into deep neural networks. In *Proc. of ICMR*, pages 269–277, 2017.

[36] Jiangfeng Wang, Hanzhou Wu, Xinpeng Zhang, and Yuwei Yao. Watermarking in deep neural networks via error back-propagation. *Electronic Imaging*, 2020(4):22–1, 2020.

[37] Siyue Wang, Xiao Wang, Pin-Yu Chen, Pu Zhao, and Xue Lin. Characteristic examples: High-robustness, low-transferability fingerprinting of neural networks. In *Proc. of IJCAI*, pages 575–582, 2021.

[38] Tianhao Wang and Florian Kerschbaum. Attacks on digital watermarks for deep neural networks. In *Proc. of ICASSP*, pages 2622–2626, 2019.

[39] Le Ya and Xuan Yang. Tiny imagenet visual recognition challenge. *CS 231N*, 7(7):3, 2015.

[40] Peng Yang, Yingjie Lao, and Ping Li. Robust watermarking for deep neural networks via bi-level optimization. In *Proc. of ICCV*, pages 14821–14830, 2021.

[41] Hongyi Zhang, Moustapha Cissé, Yann N. Dauphin, and David Lopez-Paz. mixup: Beyond empirical risk minimization. In *Proc. of ICLR*, 2018.

[42] Jialong Zhang, Zhongshu Gu, Jiyong Jang, Hui Wu, Marc Ph. Stoecklin, Heqing Huang, and Ian M. Molloy. Protecting intellectual property of deep neural networks with watermarking. In *Proc. of AsiaCCS*, pages 159–172, 2018.